Electric-field-induced migration of oxygen ions in epitaxial metallic oxide films: Non-Debye relaxation and 1/*f* noise

Arindam Ghosh* and A. K. Raychaudhuri
Department of Physics, Indian Institute of Science, Bangalore 560 012, India
(Received 30 December 2000; revised manuscript received 31 May 2001; published 23 August 2001)

We have investigated the kinetics of current-induced change of resistance and conductivity noise in thin epitaxial metallic films of $LaNiO_3$. The resistance of the film changes at a very low current (threshold current density $J_{th} \sim 10^3$ A/cm^2). We find that the time dependence associated with the change of resistance shows a stretched-exponential-type dependence at lower temperature. Above a certain temperature scale T^* (≈ 350 K), this crosses over to a creep-type behavior. At $T \sim T^*$, the time scale shows a drastic drop in the magnitude, and a long-range diffusion sets in, which leads to an increase in the conductivity noise. The phenomenon is like a ''glass-transition'' in the random lattice of oxygen ions. We observe that the stretched exponential relaxation function, as obtained from time dependence of resistivity change, can explain the spectral structure as well as the temperature dependence of the low-frequency conductivity noise. The frequency and temperature dependence of noise could clearly identify the various processes, which had been seen in the current-stressing experiments carried out in the time domain. This establishes a quantitative link between the dynamics of current-induced resistivity changes and the conductivity noise. Both the phenomena are direct consequences of the low-frequency dynamics associated with the migration of the oxygen ions. Though done in the specific context of oxide films (used in oxide electronics), this observation has a generic aspect, and the treatments developed here can be used for establishing a quantitative link between electromigration current stressing and the conductivity noise in other metallic interconnects as well.

DOI: 10.1103/PhysRevB.64.104304 PACS number(s): 66.30.Qa, 72.70.+m, 66.30.Lw, 64.70.Pf

I. INTRODUCTION

In recent years, metallic oxides like $LaNiO_3$, $RuSrO_3$, $La_{0.5}Sr_{0.5}CoO_3$, etc. are being used as interconnects or electrodes in the field of oxide electronics. Most of these oxides belong to the ABO_3 class of oxides, which are structurally similar to high T_c superconductors. Oxygen is a particularly mobile entity in many of these oxides, and the activation energy for diffusion is often $\lesssim 1$ eV.[1,2] The high mobility of oxygen species can lead to two generic problems in the use of these oxides as interconnects or electrodes in electronic applications. First, the conductivity noise in these systems can be substantially large, which mainly arises from long-range diffusion of oxygen.[3] The second problem is that the current or field induced changes in the resistivities of the films can occur over a prolonged period. This phenomenon of current-induced resistance change, which arises due to electromigration of oxygen ions has been seen before in films of $YBa_2Cu_3O_7$ in which oxygen is the mobile species.[4,5] These problems are of concern because they can seriously limit the applications of metallic-oxide films and cause reliability-linked problems. At somewhat longer current-stressing time ($t \gtrsim 100$ h), for current density $J \sim 10^5 - 10^6$ A/cm^2, the $YBa_2Cu_3O_{7-\delta}$ thin films grown epitaxially on $SrTiO_3$ and $LaAlO_3$ fail as a result of electric-field-induced stress. Microscopy studies showed large-scale material displacement at the failed region—similar to that observed in conventional metallic films during electromigration failure.[5] The electric-field-induced resistance changes and eventual failure are associated with long-range diffusion, which is expected to show a characteristic kinetics. Though the migration of oxygen ions under an applied electric field has been studied in films of high-T_c cuprates before, not much has been done to explore the kinetics of the migration, in particular, the temperature dependence of the kinetics. Another issue that is closely related to the dynamics of the migration of oxygen ions is the existence of rather high conductivity noise (or excess noise) in the oxide films. The power-spectral density of the conductivity noise in these systems has a $1/f$ form.[3,6,7] It has been shown recently that the onset of long-range diffusion of oxygen in these materials leads to enhancement of the conductivity noise.[3] This also changes the spectral structure of noise from $1/f$ (expected for broad-energy distribution of localized fluctuators) to $1/f^{3/2}$ (expected for diffusing fluctuators). In this paper we have established a quantitative connection between these two phenomena through an investigation of the dynamics associated with oxygen migration.

We did the experiments on epitaxial films of a typical normal metallic oxide $LaNiO_{3-\delta}$, which has a cubic ABO_3 structure. The material is metallic in stoichiometric form ($\delta = 0$), and its electrical properties have been investigated extensively.[8,9] Our choice of $LaNiO_{3-\delta}$ as a material for this study has been prompted by the following factors.

(1) It is a good metallic oxide in which the oxygen is fairly mobile like that in some of the high-T_c cuprates. However, it has a much simpler structure and it is isotropic, unlike the cuprates. This makes the material a simple model material to study these phenomena. It is also used extensively as an interconnect in oxide electronics.

(2) Most of the observable changes that we want to study occur close to the room temperature and in finite-time scales (typically $\sim 10^4$ sec). The threshold current density is also fairly low, $J_{th} \approx 10^3 - 10^4$ A/cm^2.

 ©2001 The American Physical Society

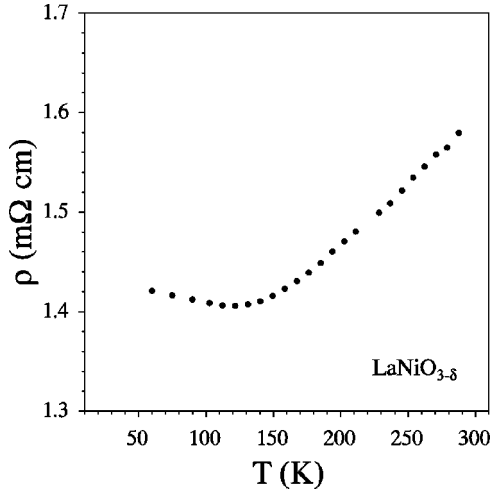

FIG. 1. Temperature dependence of resistance of a typical film of $LaNiO_{3-\delta}$ studied in this investigation. The estimated $\delta \approx 0.1$.

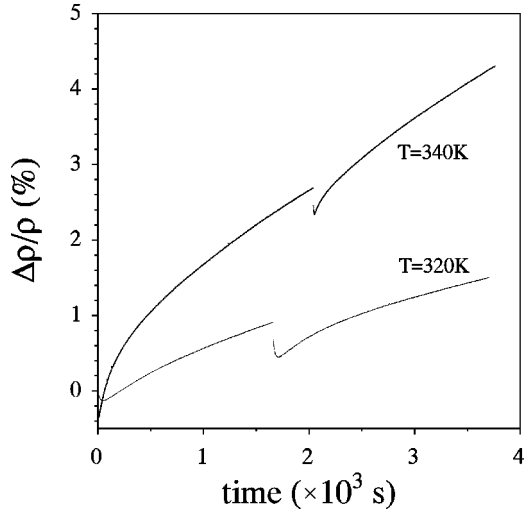

FIG. 2. A typical resistivity change $(\Delta\rho/\rho)$ vs time curve seen at two temperatures for a measuring current density $J=4\times10^4$ A/cm^2. The resistance shows an initial decrease on initiation and reversal of the current (termed as *r* process). This is followed by a slow increase in ρ termed as *d* process (see text).

In perovskite oxides with $ABO_{3-\delta}$ structure, at room temperatures and at normal pressure, $\delta=0$ may not represent the equilibrium oxygen stoichiometry. For a given value of δ, if it is not the equilibrium value, the system will try to attain equilibrium, but will be kinetically frozen. This will give rise to a slow dynamics in the system. The conductivity noise is likely to probe this dynamics. This dynamics will also be at the basis of any time dependence that will be associated with any driven migration of oxygen ions/vacancies. This is the central issue addressed in the present investigation. We find that the observed conductivity noise has a direct relation with the dynamics of electric-field-induced migration.

II. EXPERIMENT

All the experiments reported here are done with thin epitaxial films (thickness $\approx$150 nm) of $LaNiO_{3-\delta}$ grown on $LaAlO_3$ substrate by pulsed-laser ablation. Details of growth and characterization has been given elsewhere.[10,11] The films used here have a room-temperature resistivity, $\rho_{rt}\sim1-1.6$ mΩ cm. The films were patterned for resistance and noise measurements. The resistance measurements were done using a low-noise bridge with a precision of 1 ppm. The noise measurements used a five-probe geometry[12] and phase-sensitive detection. Measurements showed excellent reproducibility down to spectral power as low as $\lesssim10^{-19}$ V^2/Hz. This has been achieved by implementing extensive digital-signal-processing techniques. The patterned films for noise detection had an active volume $\Omega\approx5\times10^{-8}$ cm^3. The details are given elsewhere.[13] All the data are taken at thermal equilibrium where the temperature was controlled to within ±5 mK.

III. RESULTS

A. Field-induced changes in resistance

In Fig. 1 we show the change in ρ as a function of T for a typical film used in this investigation. The data are taken using a small measuring current so that $J\ll J_{th}$. The film is metallic and resistance shows a minimum at 130 K similar to disordered systems with weak electron localization. Typical δ of the films were determined by comparing their resistivity with bulk samples in which δ can be directly detected by quantitative chemical means.[8] For the films studied, the estimated $\delta\approx0.08-0.1$.

Typical resistance R vs time t data showing current-induced changes are plotted in Fig. 2. Immediately after applying the current, R drops slightly in a scale of few minutes. Then it starts to increase after passing through a minimum. We call this increase in R the ''damage'' (*d*) process. Over several hundred minutes, R changes by about $\sim2-3$ % depending on the temperature and the current density J. Then the current was reversed. On reversal of current, R falls again typically by $\lesssim1$% and then starts to increase again after passing through a minimum. We call this drop in R the ''recovery'' (*r*) process. The time scale involved in the *r* process is much smaller than that involved in the *d* process, and it is quite similar to the early resistance drop seen on initial application of the current. The choice of the names *r* process and *d* process has no specific reason other than the fact that when R drops, some defects are expected to get annealed out indicating a ''recovery'' while the opposite is true for the ''damage'' process.

Similar *r* and *d* processes were seen in epitaxial films of high-T_c cuprates at room temperature.[4] It was concluded that the resistance change is a consequence of the oxygen-ion migration and while the *r* process heals defects, the *d* process increases the defects and disorder. This similarity of the transport kinetics, however, does not necessarily imply the same underlying physical process in both the materials, although oxygen-ion migration lies at the origin in both. The current-stressing experiments were done for $270\text{ K}<T<400$ K. From the data shown at three characteristic temperatures in Fig. 3, it is very clear that both *r* and *d* processes become faster as T is raised. The *r* process becomes so fast

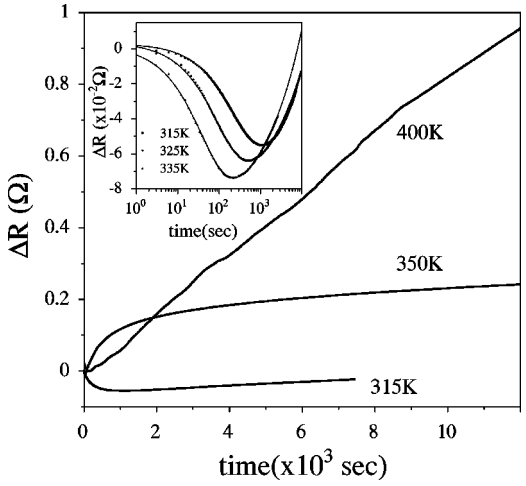

FIG. 3. A resistivity change occurring over a longer time scale. The processes become faster as T is increased. A creeplike resistance change $\Delta R_{creep} \propto t$ appears for $T \gtrsim 350$ K, and dominates the time dependence for $T=400$ K. The inset shows the fit to the data for some characteristic temperatures to Eqs. (2)–(4).

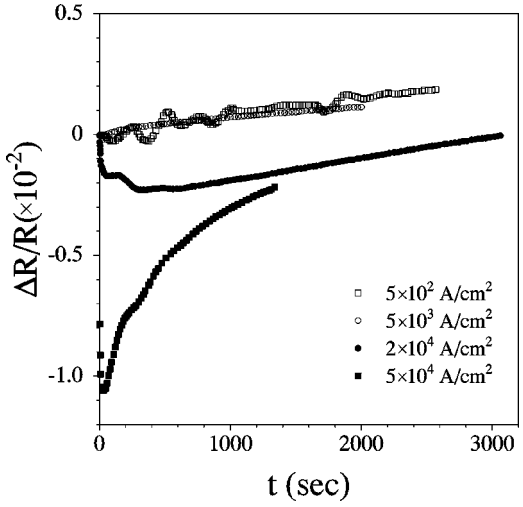

FIG. 4. Dependence of the fractional resistance change ($\Delta R/R$) on measuring current. At the lowest measuring current ($J=5\times10^2$ A/cm^2), the slow change in resistance is accompanied by an oscillatory change, which is absent at highest currents. Data is taken at $T=340$ K.

for $T \gtrsim 350$ K, that it is barely visible in the scale of our experiment. This can be seen in the data for $T=350$ K and 400 K. The resistance change in both r and d processes, have stretched-exponential dependence on time. However, for $T \gtrsim 350$ K, the time dependence becomes very fast and gets a creeplike component with linear dependence on time ($\Delta R/R \propto t$). A detailed analysis of the time dependence will be done later on.

B. Threshold current density

The measurements shown in Fig. 2 were made with a current of 80 mA. This corresponds to a current density $J \approx 4\times10^4$ A/cm^2 and an electric field $E \approx 80$ V/cm. J was so chosen that it was not too high to cause an immediate rupture, and at the same time not so low that no perceptible change occurs. We find that there is a threshold current density J_{th} associated with both the recovery and damage processes. We have investigated this in detail at $T \approx 340$ K where both processes are perceptible. In Fig. 4 we show the resistance change as a function of time for four current densities. At a current density $J \approx 5\times10^2$ A/cm^2 there is a slow change in the resistance as a function of time but it has an oscillating component with $\Delta R/R \approx 10^{-3}$ riding on the slow increase. This oscillation is not an experimental noise because it is much larger than our resolution ($\sim 1-10$ ppm) and it vanishes for $J \gtrsim 10^3$ A/cm^2. At even lower current density $J \approx 5\times10^1$ A/cm^2, there is no change in R with t within our detection limit. To clearly see how the relative change, $\Delta R/R$, associated with both r and d processes depends on J, we have plotted $\Delta R/R$ as a function of J in Fig. 5 as obtained from a typical R vs t plot. The initial dip in R when the current is reversed is taken as a measure of the r process (marked as ΔR_1 in the inset of Fig. 5). After the initial drop, the resistance attains a minimum and increases again due to the d process. We took the change in R from the minimum, over a period of 1800 sec, as a measure of the d process. This is marked as ΔR_2. A more quantitative analysis by fitting the data to a time-evolution function has been done later on. It can be seen in Fig. 5 that for $J \gtrsim 10^3$ A/cm^2, $(\Delta R/R)_1$ depends strongly on J. For $J \gtrsim 10^5$ A/cm^2, a prolonged current stressing for $t > 24$ h leads to permanent failure. For $J < J_{th}$, we observe an oscillation in R.

A very small but perceptible d process shows up even at a very low current as can be seen in Fig. 5. $(\Delta R/R)_2 \approx 10^{-3}$ for $5\times10^2 < J < 2\times10^4$ A/cm^2. For $J \gtrsim 2\times10^4$ A/cm^2 $(\Delta R/R)_2$ increases very rapidly. We take this as the J_{th} for substantial d process. For comparison, the value of J_{th} is much less than that seen in high T_c cuprates ($J_{th} \gtrsim 10^5$ A/cm^2) as well as that seen in metallic films. In-

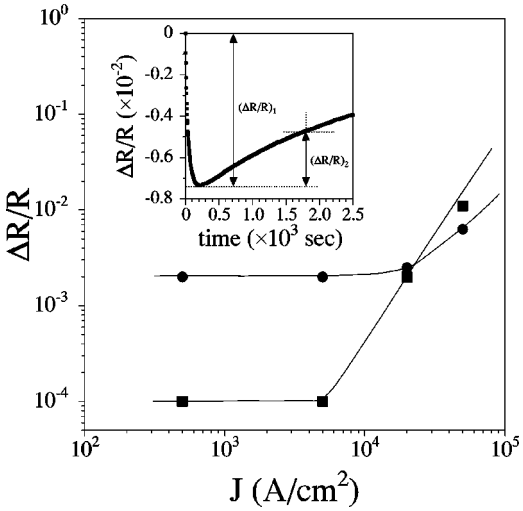

FIG. 5. Dependence of $\Delta R/R$ on measuring current showing the existence of a threshold current density J_{th} for both r and d processes. The data for the r process is obtained from ΔR_1 and that for the d process from ΔR_2 as stated in the text. Lines are guides to the eye. Inset: The scheme of calculating ΔR_1 and ΔR_2 (see text).

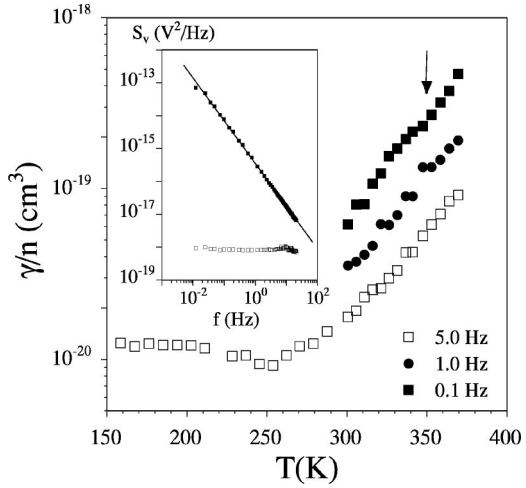

FIG. 6. Temperature dependence of the scaled noise γ/n as a function of T for three frequencies. The appearance of a shallow plateau in the noise at $T \approx 350$ K at lower frequencies ($f \lesssim 1$ Hz) can be noted. The inset shows the $1/f^{\alpha}$ nature of the measured spectral power and the background (open squares), which is mainly the $4k_BTR$ thermal noise.

terestingly, the exact value of J_{th} depends on oxygen content δ as well as on T. In this paper, in order to keep the issues addressed to within a meaningful limit, we used films of very similar δ. We just note that as $\delta \rightarrow 0$ (i.e, in well-oxygenated films), J_{th} decreases severely.

C. Low-frequency conductivity noise or "1/*f*" noise

It is well known that the excess noise or conductivity noise, which often has a spectral power dependence $S(f) \propto 1/f^{\alpha}$ ($\alpha \sim 1$), can probe the long-time (low-frequency) dynamics of the scatterers that make strong contribution to ρ. The electric-field-induced resistance change is due to electromigration of oxygen ions. The slow dynamics of diffusion of oxygen results in large characteristic time scales. Past studies in this material have shown that the resistivity strongly depends on the oxygen defects. In that case the slow dynamics associated with oxygen migration (which is a vacancy-mediated migration), or even local rearrangements, will give rise to low-frequency conductivity fluctuations. Thus a study of noise can complement the electromigration experiment, because both of them are expected to arise from the same process. More importantly, we would like to explore whether a quantitative connection can be established between the dynamics probed in the time domain by the current stressing experiment and that probed by the noise experiment in the frequency domain.

In Fig. 6 we show the temperature dependence of the spectral power of the observed noise as a function of T. We have expressed the spectral dependence of noise as

$$\frac{\gamma(f)}{n} = \frac{f S_V(f) \Omega}{V^2}, \tag{1}$$

where n is the carrier density, $S_V(f)$ is the spectral power of voltage fluctuations at a frequency f and bias V, measured in a sample of volume Ω. Traditionally, the dimensionless parameter γ is called Hoog's parameter.[14] However, we do not attach much significance to it other than being a convenient way to normalize the noise data. The quantity γ/n is directly calculable because all the quantities in the right-hand side of Eq. (1) are obtained from experiment. The inset of Fig. 6 shows the $1/f^{\alpha}$ nature of the spectral power density. The background noise, which is predominantly $4k_BTR$, is also shown in the inset. γ/n increases as T increases. At $T \approx 340$–350 K it shows a shallow plateau and it increases again at a faster rate for $T \gtrsim 350$ K. The shallow plateau becomes more visible at lower frequency. (See the data at 0.1 Hz.) It is to be emphasized that the plateau is reproducible and has been seen in many samples. We will see below that at $T \approx 350$ K, the time scales associated with the kinetics of ion migration undergo a rather sharp change. The rise in noise at this temperature is a signature of this change.[3] A detailed quantitative analysis of the temperature dependence of noise is given in the discussion section below (see Fig. 14).

IV. DISCUSSION

A. Kinetics of resistivity change

In order to obtain quantitative evaluation of the time scales, we first fitted the $\Delta R(t)[=R(t)-R(0)]$ vs t data to the following functional form:

$$\begin{aligned}\Delta R(t) &= \Delta R_r(t) + \Delta R_d(t) \\ &= \Delta R_{0r}[1 - e^{-(t/\tau_r)^{\beta_r}}] + \Delta R_{0d}[1 - e^{-(t/\tau_d)^{\beta_d}}] + \nu t,\end{aligned} \tag{2}$$

where the subscripts refer to the r process and the d process. Both $\Delta R_r(t)$ and $\Delta R_d(t)$ follow stretched-exponential dependence on time t. For $\Delta R_d(t)$, a creep component ($\propto t$) shows up at $T \gtrsim 350$ K, and dominates the time dependence at higher T. This component enters additively as $\Delta R_{creep} \approx \nu t$ in the expression for $\Delta R_d(t)$, where $\nu \approx 0$ for $T \lesssim 350$ K. At low temperatures ($T \lesssim 330$ K), τ_d is very large compared to the measurement time t, and hence

$$\Delta R_d(t) \approx (t/K)^{\beta_d} \tag{3}$$

for $\tau_d \gg t$, where

$$K = \frac{\tau_d}{(\Delta R_{0d})^{1/\beta_d}}. \tag{4}$$

The data are fitted to Eqs. (2)–(4) and the parameters are obtained. [Equations (3) and (4) were used till $T = 340$ K. Beyond that we used the full expression given by Eq. (2).] The inset of Fig. 3 shows a few fits to the data as obtained using the equations above. Figure 7 shows a plot of $\Delta R_d(t)$ vs t to show the t^{β_d} dependence for the d process, as expected from Eq. (3).

The time scale for the recovery process, τ_r, follows an Arrhenius dependence on T [$\tau_r = \tau_{0r} \exp(E_r/k_BT)$] with an activation energy $E_r \approx 0.84$ eV and $\tau_{0r} \approx 1.2 \times 10^{-11}$ sec. This is shown in Fig. 8. The activation energy deduced from

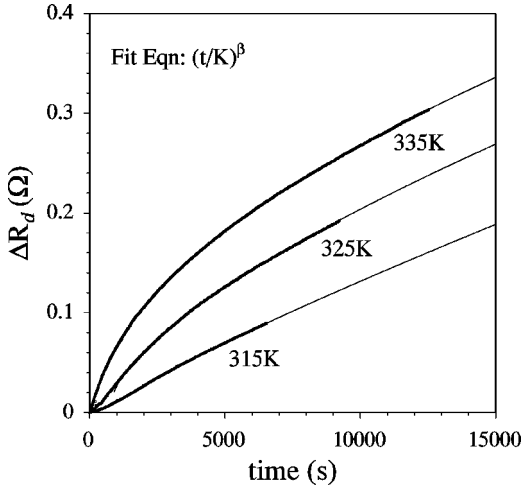

FIG. 7. The time dependence of the resistance change in the *d* regime. Fits to the data use Eq. 3.

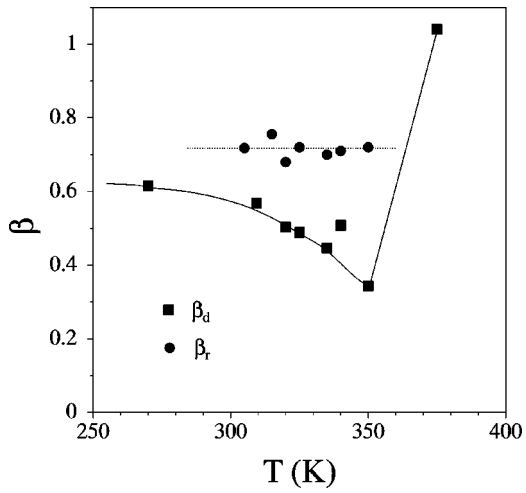

FIG. 9. Temperature dependence of the exponent β_d and β_r. Note that while β_r is essentially T independent, β_d shows a sharp change at $T=T^*\approx 350$ K. Lines are guides to the eye.

the temperature dependence of τ_r is the same as that seen for oxygen migration from other techniques like diffusion experiments[2] as well as from simulation studies.[15] This shows that the process of current-induced change in R has its origin in oxygen-ion migration. The value of $\Delta R_{0r}/R\approx 1\%$ are nearly temperature independent for $T\lesssim 335$ K. The exponent β_r is essentially temperature independent, and has a value $\beta_r\approx 0.7$ for the films studied by us (see Fig. 9). β_r depends strongly on the oxygen-defect δ and as $\delta\rightarrow 0$, $\beta_r \rightarrow 0.5$. Presumably, when the film is nearly fully oxygenated ($\delta\rightarrow 0$), the migration of oxygen will involve a correlated relaxation of a larger length scale because the average separation of oxygen-defect sites is larger. This will give rise to a sequential process, which makes the relaxation strongly non-Debye type ($\beta_r\lesssim 0.5$).

The temperature dependence of τ_d is shown in Fig. 10. In this case we show the temperature dependence of K [see Eq. (4)], which in turn shows the T dependence of τ_d, since the T dependence of ΔR_{0d} is less severe. It has a relatively weak temperature dependence for $T\lesssim 340$ K. However at $T\approx 350$ K, K drops substantially. From the limited temperature range we can get a very approximate estimate for the temperature dependence of τ_d, which is found to follow an Arrhenius relation with an activation energy $E_d\approx 0.7$–0.8 eV, and an attempt time constant $\tau_{0d}\approx 6\times 10^{-10}$ sec. E_d essentially has the same value as E_r within our experimental uncertainty and $\tau_{0d}/\tau_{0r}\approx 50$.

In Fig. 10 we have also shown the T dependence of the creep rate ν. This is small near $T=350$ K and its contribution to the observed resistance change increases rapidly at higher T. We thus make the interesting observation that at $T\approx 350$ K there is a crossover from a stretched-exponential-type relaxation at lower temperature to a creep-type relaxation at higher temperature. The creep rate also follows an Arrhenius temperature dependence with activation energy $E_{creep}=0.8$ eV. This again is similar to E_r and E_d and all

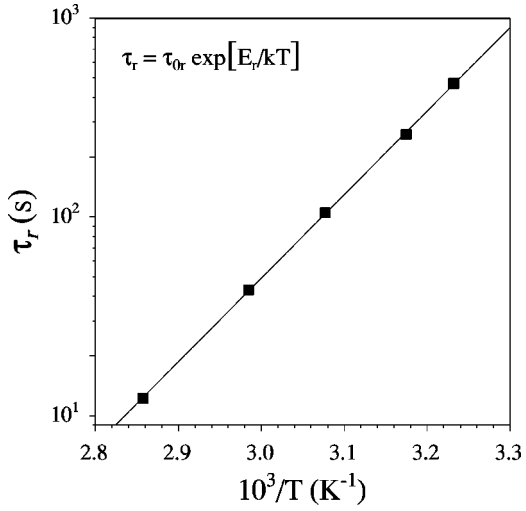

FIG. 8. Arrhenius temperature dependence of the relaxation time τ_r on T. The estimated activation energy $E_r\approx 0.84$ eV.

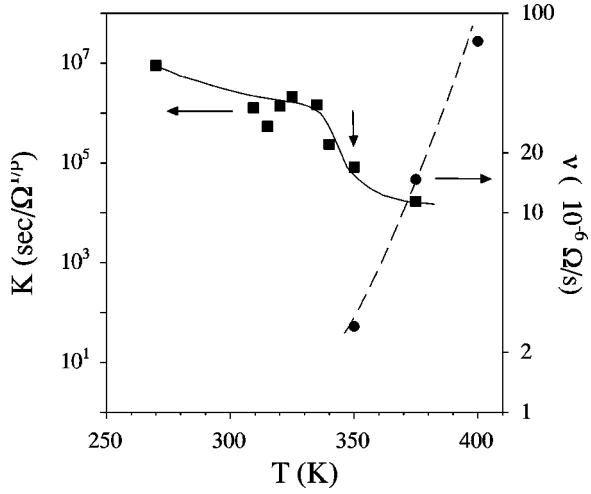

FIG. 10. Temperature dependence of the time scale τ_d ($\propto K$) and the creep rate ν, as obtained from the data using Eqs. (2)–(4) (see text). The drop in K and the rapid rise of ν at $T\approx 340$ K can be noted. Lines are guides to the eye.

these are similar to the activation energy for oxygen-ion migration. Thus the physical mechanism underlying the resistance change in both the processes is related to the migration of oxygen ions. The stretched-exponential exponent β_d is shown in Fig. 9. In contrast to β_r, β_d has a sharp temperature dependence, particularly close to 350 K. We shall discuss the implication of this in the next section.

B. Glasslike freezing: Its implication on stability of oxide films

The onset of creeplike change in R as a function of t for $T \gtrsim 350$ K signals the onset of long-range diffusion. Below this temperature, long-range diffusion is frozen in. The situation is thus similar to the process of glass transition, where at a certain characteristic temperature range the long-range diffusion kinetically freezes out on cooling. One can think of this phenomenon as kinetic freezing of long range diffusion (''glass transition'') in the oxygen lattice. Evidence of a glass-transition-like freezing in the oxygen lattice at $T^* \approx 350$ K can also be seen in the T dependence of the stretched-exponential exponent β_d (Fig. 9). The value of the exponent β_d is high in the ''molten'' state ($T > T^* \approx 350$ K), which signifies a nearly Debye-type relaxation associated with the oxygen migration. However, in the frozen state ($T \lesssim 350$ K), the value of β_d sharply decreases to ≈ 0.4–0.6 implying a hierarchy of the relaxation process, similar to that in the frozen state of a structural glass.[17] Interestingly, in a recent noise study at low temperatures ($T < 20$ K),[16] we found clear evidence of low-energy two-level systems in this material, as generally observed in conventional glasses.[18] In that study we were able to conclude that these ''glasslike'' low-energy excitations occur in the randomly frozen lattice of oxygen ions. The observation of kinetic freezing at $T^* \approx 350$ K thus very well connects to the observation of low-energy excitations in these solids. (Note: As δ is varied, the oxygen stoichiometry is changed, the parameters describing the electromigration also change, and when $\delta \to 0$, T^* decreases substantially.)

We find that $\tau_d \gg \tau_r$ at all temperatures for $T < T^*$. Well within the frozen range ($T \ll T^*$), $\tau_d/\tau_r \gtrsim 10^3$ and close to T^* the ratio drops to ~ 10. This has an interesting analog in the relaxation in structural glasses. In structural glasses, the relaxation involving large-scale structural rearrangements (called the α relaxation) takes place for $T \gtrsim T_g$, the glass-transition temperature. While $T < T_g$ this freezes out and the relaxation (called the β relaxation) takes place by localized atomic rearrangement. In our case also we feel that the r process, like β relaxation, involves localized atomic rearrangements while the d process, like α relaxation, involves the long-range migration.[17]

The effect of long-range diffusion for $T \gtrsim 350$ K can also be seen in the conductivity noise in Fig. 6 as discussed earlier. One can see that at the onset of the long-range diffusion, the temperature dependence of the noise shows an upturn. The fact that the extra noise observed at $T \gtrsim 350$ K arises from the long-range diffusion has been discussed in detail in subsequent sections. We also find that in this temperature range the spectral structure of the noise changes. Though the spectral power retains its approximate $1/f^{\alpha}$ character, α changes from ≈ 1.2 for $T \lesssim 350$ K to $\alpha \to 1.5$ for $T \gtrsim 350$ K. At even higher temperature ($T \gtrsim 370$ K) the exponent becomes nearly $\alpha \approx 2.0$ for $f \lesssim 10^{-2}$ Hz. This has been discussed in detail later on.

The observation of a glasslike freezing of the oxygen migration is a new result. Interestingly, there exists evidence from calorimetric studies of glass-transition-like phenomena associated with the excess oxygen in a related compound La_2NiO_4.[19] We feel that this new phenomenon will be extremely important in determining the reliability and stability of oxide films as interconnects or electrodes. The important lesson from our investigation is that if these oxide interconnects have to be used in application with low noise and stability against field-induced oxygen-ion migration, the characteristic temperature T^*, where the''glass-transition'' of oxygen lattice occurs, should be as large as possible, preferably much above the temperature range of application. For $T \lesssim T^*$, the change in R is small and the noise is low. For $T \gtrsim T^*$, one expects long-range migration to take place leading to large-scale transport of matter, which will lead to substantial change in R, significantly high noise and eventual failure of the film.

C. Physical process and structural aspects

Perovskite oxide ABO_3 has a structural frame work, which is not made up of a close oxygen packing, unlike structures of corundum or spinel-type oxides. This allows high mobility of oxygen ions. Experiments on a broad class of ABO_3 oxides have shown that the diffusivity of the cations is very small compared to that of the oxygen.[1,2] Recent molecular-dynamics simulations in ABO_3 have corroborated with this.[15] The diffusion constant $\mathcal{D}$ of oxygen follows the Arrhenius relation $\mathcal{D} = \mathcal{D}_0 \exp(-E_a/k_B T)$. The activation energy measured from diffusion experiments and simulations gives $E_a \approx 0.6$–0.8 eV. This is the same as that measured by us from the noise as well as the electromigration experiments. In these materials the typical $\mathcal{D}_0 \approx 10^{-4} - 10^{-5}$ cm^2/sec^2. The typical τ_{0r} associated with r process is $\approx 1.2 \times 10^{-11}$ sec. Thus the root-mean-square displacement of oxygen in the r process $\langle x_0^2 \rangle^{1/2} \approx (6 \mathcal{D}_0 \tau_{0r})^{1/2} \approx 0.3$–$0.9$ nm$\approx (0.8$–$2.5) a_0$, where a_0 is the cubic lattice constant. Thus the movement of atoms in the r process is localized to within only a few unit cells.

D. Stretched-exponential correlation function and low-frequency noise

In this section we establish that the stretched-exponential relaxation function $\phi(t)$, which determines the non-Debye relaxation observed in the field-induced resistance change, also governs the low-frequency conductivity noise. Our noise measurement was carried out over $10^{-3} < f < 10^2$ Hz, corresponding to a time scale spanning approximately over 10^{-3}–10^2 sec. Since $\tau_d > \tau_r$, at a given temperature T we expect the d process to be important for noise in the lower-frequency regime, whereas the r process governs the high-frequency part. However, close to T^* the d process also becomes faster, and one expects significant contribution to the

noise spectrum from both the processes over the entire experimentally observed frequency range.

From Eq. (2), we find that for both processes the relaxation function $\phi(t,\tau)$ is a stretched exponential, i.e., $\phi_x(t,\tau)=\exp[-(t/\tau_x)^{\beta_x}]$, where $x=r,d$. In the analysis for noise, we assume $\phi_x(t,\tau)=\exp[-(t/\tau)^{\beta_x}]$, where τ is a distributed quantity with mean $\langle\tau\rangle\approx\tau_x$ and width σ_x. (τ_x is obtained as the effective time scale in the electromigration-induced resistivity change.) If the processes are statistically independent, the noise from them will be additive, and the total noise $S(f,T)=S_r(f,T)+S_d(f,T)$. Using the stretched-exponential autocorrelation function, we get[20,21]

$$S_x(f,T)=C_1\int_0^\infty d\tau\,\rho_x(\tau,T)\int_{-\infty}^{+\infty}dt\,e^{-j(2\pi ft)}e^{-(t/\tau)^{\beta_x}}$$

$$=C_1\int_0^\infty d\tau\,\rho_x(\tau,T)\,\tau Q_{\beta_x}(2\pi f\tau), \tag{5}$$

where C_1 is a constant independent of f and T, $\rho(\tau,T)$ is the distribution function for the relaxation time τ, and $Q_\beta(z)$ is the Levy function expressed as[21]

$$Q_\beta(z)=\frac{1}{\pi}\sum_{n=1}^{\infty}\frac{(-1)^{n+1}}{n!}\frac{\Gamma(1+\beta n)}{z^{1+\beta n}}\sin(\pi\beta n/2). \tag{6}$$

If we assume the diffusing species to be mutually independent, the most natural choice for the distribution function $\rho_x(\tau,T)$ is the log-normal distribution.[21] We thus have

$$\rho_x(\tau,T)d\tau=\frac{1}{\sigma_x\sqrt{2\pi}}\exp\left[-\frac{\ln^2(\tau/\tau_x)}{\sigma_x^2}\right]d\ln(\tau/\tau_x). \tag{7}$$

The temperature dependence of $\rho(\tau,T)$ comes from that of τ. Using Eqs. (5), (6), and (7), we can calculate the frequency and temperature dependence of the spectral power density $S(f,T)$. The values of β_x and τ_x ($x=r$ and d for the r and d process, respectively) are obtained experimentally from the electromigration-induced resistance changes. If the temperature dependence of $\tau_x(T)$ is known, we can also calculate the temperature dependence of noise. The only unknown parameter is the width of the τ distribution, σ_x, which is independent of T. We can thus determine the constants C_1 and σ_x at a specific T and use those values to quantitatively estimate $S(f,T)$ at all f and T.

Certain asymptotic limits of Eq. (5) are worth noting. In the absence of a distribution of τ, i.e., $\sigma_x\to 0$, for $f\gg\tau_x^{-1}$, we have $S(f)\sim 1/f^{1+\beta_x}$. It is interesting to note that for the Debye case $\beta_x=1$, and one obtains $1/f^2$ dependence of $S(f)$. Only in the limit of extreme non-Debye case ($\beta_x\to 0$), $S(f)$ tends to the $1/f$ form. For an intermediate β_x, one thus needs a finite nonzero σ_x to obtain $S(f)\sim 1/f^\alpha$ with $\alpha\approx 1$ or close to it.

In Fig. 11, we show the power-spectral density $S(f)$ of the low-frequency resistance fluctuations in one of the $LaNiO_{3-\delta}$ films recorded at $T=310$ K. At this temperature, the parameters of the r process are $\beta_r=0.70$ and $\tau_r=\tau_{0r}\exp(E_r/k_BT)\approx 115.9$ sec. The solid line shows the calculated frequency dependence with $C_1=1.1\times 10^{-13}$ and $\sigma_r=7.0$. Clearly, the fit is very good for $f\gtrsim 0.05$ Hz. For $f\gtrsim 0.05$ Hz the predominant contribution to noise is thus from the r-process. For $f\lesssim 0.05$ Hz, the calculated noise (based on the r process alone) is lower than the actually observed noise. In Fig. 11, the frequency dependence of noise in this regime is shown by the dotted line, having the functional form of $S(f)\sim 1/f^{3/2}$. For the d process, $\beta_d\approx 0.5$. Moreover, at $T=310$ K, the time scale for the d process $\tau_d\gg\tau_r$, f_{min}^{-1}, where f_{min} is the minimum frequency of the recorded spectrum. As mentioned before, in this limit $S(f)$ takes the asymptotic form, $S_d(f)\sim 1/f^{1+\beta_d}\sim 1/f^{3/2}$ when $\sigma_d\to 0$. Thus we identify the extra noise in the regime $f\lesssim 0.05$ Hz as a contribution from the d process. It is interesting to note that for the d process, the distribution width σ_d of $\rho_d(\tau,T)$ is extremely narrow ($\sigma_d\to 0$), in contrast to the r process, which has a significantly larger spread in τ. The inset to Fig. 11 shows the combined fit over the entire observed spectrum taking both processes into account. The agreement is clearly excellent over 5 decades in frequency.

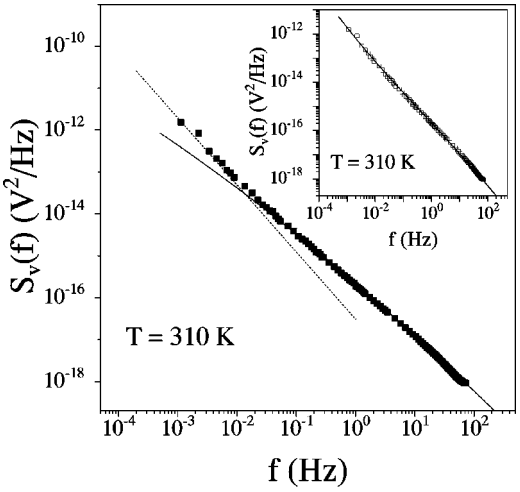

FIG. 11. Frequency dependence of low-frequency conductivity noise recorded at $T=310$ K. The solid line is the fit to the data using Eqs. (5), (6), and (7) with the parameters for the r process. The dotted line plots the function $S_V(f)\propto 1/f^{3/2}$. The inset shows the total contribution of the r and d processes.

E. Spectral signature of oxygen migration

In the following part of the paper, we would like to calculate the frequency dependence of the spectral power at different temperatures to identify the contributions of the r, d, and the creep processes to the observed noise. In Fig. 12, we have shown the experimentally observed noise at $T=290$ K, 300 K, and 320 K, along with the corresponding numerical estimation. The r process is the dominant source of noise for $f\gtrsim 0.1$ Hz in this temperature range. Throughout our calculations for the noise from the r process we have kept $\sigma_r=7.0$, as obtained from the fit at $T=310$ K. The value of C_1 was varied by $\lesssim\pm 20\%$ in order to allow for the experimental uncertainty. C_1 was also normalized by the square of the bias across the sample. In Fig. 12 (and in Fig. 13), we had to shift each spectrum in order to restore clarity

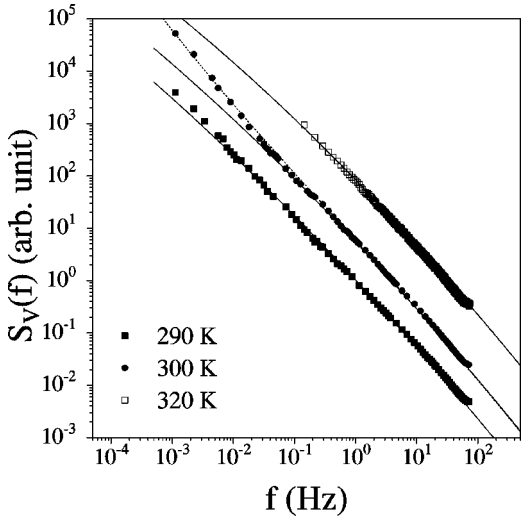

FIG. 12. Noise power spectrum in the temperature regime where the *r* process contributes predominantly. The solid lines show the *r*-process estimates using Eqs. (5)–(7) and C_1 and σ_r obtained from the fit at $T=310$ K. For $T=300$ K, the dotted line shows the total evaluation taking both *r* and *d* processes into account.

in display. Hence the data are plotted in arbitrary unit. The values of β_r and τ_r were already known from the electromigration experiments. As T decreases, the excess noise at low frequencies due to the *d* process becomes insignificant and at $T=290$ K, we have fitted the entire frequency spectrum using the parameters for the *r* process only. With increasing temperature, the *d* process also becomes faster, and one needs to take its contribution into account at lower frequencies in order to fit the entire range of observed spectrum (as shown in Fig. 11 for $T=310$ K). This is marked in the figure as dotted lines.

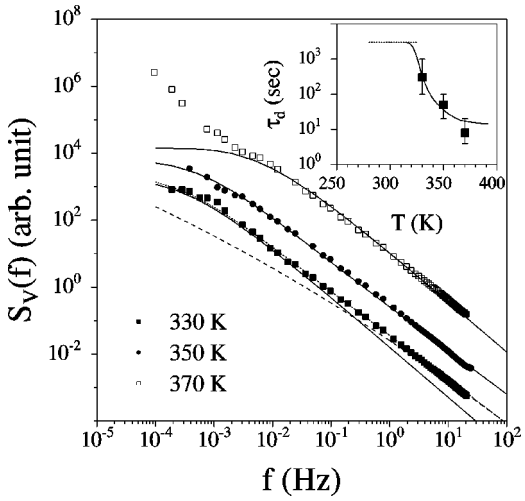

FIG. 13. Noise power spectrum in the temperature regime where the *d* process is dominant. The solid lines are fits using Eqs. (5)–(7) with the parameters for the *d* process. For $T=330$ K the dashed line shows the corresponding estimate using the *r* process. Inset shows the temperature dependence of the *d*-process time scale τ_d obtained as a fit parameter. The dotted line denotes the upper limit of τ_d.

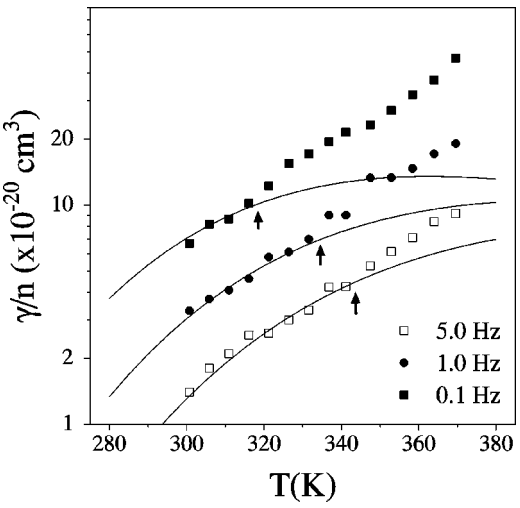

FIG. 14. Temperature dependence of the noise parameter γ/n measured at three different frequencies. The lines show the numerical estimation based on the *r*-process parameters. The arrows show the temperature at which the contribution from the *d* process exceeds that from the *r* process.

For $T\gtrsim 330$ K, the contribution in the observed noise spectrum from the *d* process becomes dominant, as shown by the solid lines in Fig. 13. At $T=330$ K, the dashed line is the estimate from the *r* process and the dotted line is the sum of the two contributions. For $T=350$ K, the contribution of the *r* process to noise is extremely small and *d*-process calculations fit the entire spectrum. Finally, at $T=370$ K, we observe significant excess noise in the frequency range $f \lesssim 0.01$ Hz. We associate this with the irreversible creeplike process as observed in the electromigration experiments at high temperatures. For $f\lesssim 0.01$ Hz the spectrum follows a $\sim 1/f^2$ dependence that can arise from the drift in R due to the creeplike process. (Note: For the *d* process $\sigma_d \approx 0.01$, which is much smaller than σ_r.) β_d is known from the electromigration experiment. However, due to the ambiguity in determination of τ_d as mentioned before, we used this as a fit parameter. The τ_d obtained from experiment is shown in the inset of Fig. 13. In the temperature range $T\sim 350$ K, there is a sharp drop in the value τ_d. This is very similar to that seen in Fig. 10.

F. Temperature dependence of noise

Thus far we have calculated the spectral structure of noise at various temperatures. We now use Eqs. (5), (6), and (7) to evaluate the temperature dependence of noise parameter $\gamma(f,T)/n$ defined in Eq. (1) for different values of f. The result is shown in Fig. 14. The lines through the data points are calculated using the parameters for the *r* process. At low frequencies ($f\lesssim 0.1$ Hz), the calculation clearly underestimates the observed noise beyond $T\gtrsim 320$ K. In this regime noise is dominated by the *d* process. As observation frequency increases, expectedly, the calculation based on the *r* process alone gives better estimate of noise at higher temperatures. The arrows in the figure identify the temperature scale at which the contribution to noise from the *d* process

becomes comparable to that due to the *r* process. (Due to nonavailability of unambiguous temperature dependence of τ_d, the same procedure as that done for the calculation of the noise from the *r* process could not be carried out for noise from the *d* process.) One can also see that there is a perceptible change in the magnitude of noise at $T \approx 350$ K and an extra noise contribution arises. This is due to the onset of the creeplike process. The temperature dependence of the noise at different frequencies thus clearly manifests the relative contribution of the various processes.

V. CONCLUSION

In this paper, we have investigated the electric-field-induced changes in metallic-oxide films and the kinetics associated with the change. This is found to be related to the migration of oxygen ions. The slow dynamics associated with this is also the source of conductivity noise in this material. We found that the temperature dependence of the time scales associated points towards a glasslike freezing in the oxygen lattice. The issue of stability of thin metallic-oxide films towards electromigration is an important issue from the technological application of these films in oxide electronics. This investigation is focused on some of the generic science questions that lie at the core of this problem.

The spectral structure of the noise spectrum, as well as the *T* dependence, have been calculated from the relaxation function observed in the electromigration experiment. It is indeed gratifying to observe that one can evaluate the noise from the time-domain data obtained from an independent experiment. Though done in the context of an oxide film, the procedure followed for both experiment and numerical evaluation is sufficiently general, and should be applicable for other related studies as well. We believe that establishing a direct quantitative link between the electromigration dynamics and the noise spectra will make noise a viable tool to study the structural and electrical stability of thin films.

ACKNOWLEDGMENTS

The authors wish to thank Dr. R. Sreekala, Dr. M. Rajeswari, and Professor T. Venkatesan of the Center of Superconductivity Research, University of Maryland for providing the high-quality $LaNiO_{3-\delta}$ films used in this work. A.G. acknowledges the help of Swastik Kar during the preparation of this manuscript.

*Present address: Cavendish Laboratory, University of Cambridge, Madingley Road, Cambridge, UK.

[1] A. Reller, Philos. Mag. A **68**, 641 (1993), and references therein.

[2] T. Ishigaki, S. Yamauchi, K. Kishio, J. Mizusaki, and K. Fueki, J. Solid State Chem. **73**, 179 (1988); A. Belzner, T. M. Gur, and Robert Huggins, Solid State Ionics **57**, 327 (1992); J. Mizusaki, *ibid.* **52**, 79 (1992); S. Carter, A. Seluck, R. J. Chater, J. Kajda, J. A. Kilner, and B. C. H. Steele, *ibid.* **53-56**, 597 (1992).

[3] Arindam Ghosh, A. K. Raychaudhuri, R. Sreekala, M. Rajeswari, and T. Venkatesan, J. Phys. D **30**, L75 (1997).

[4] B. H. Moeckly, D. K. Lathrop, and R. A. Buhrman, Phys. Rev. B **47**, 400 (1993); B. H. Moeckly, P. E. Sulewski, and R. A. Buhrman, Appl. Phys. Lett. **64**, 1427 (1994).

[5] S. Vitta, M. A. Stan, J. D. Warner, and S. A. Alterovitz, Appl. Phys. Lett. **58**, 759 (1991).

[6] S. Scouten, Y. Xu, B. H. Moeckly, and R. A. Buhrman, Phys. Rev. B **50**, R16 121 (1994).

[7] L. Liu, K. Zhang, H. M. Jaeger, D. B. Buchholz, and R. P. H. Chang, Phys. Rev. B **49**, 3679 (1994).

[8] N. Gayathri, A. K. Raychaudhuri, X. Xu, J. L. Peng, and R. Greene, J. Phys.: Condens. Matter **10**, 1323 (1998), and references therein.

[9] N. Gayathri, A. K. Raychaudhuri, X. Xu, J. L. Peng, and R. Greene, J. Phys.: Condens. Matter **11**, 2901 (1999).

[10] K. M. Satyalakshmi, R. M. Mallya, K. V. Ramanathan, X. Xu, K. Braidnard, D. C. Gautier, N.Y. Vasanthacharya, and M. S. Hegde, Appl. Phys. Lett. **62**, 1233 (1993).

[11] M. Sagoi, Appl. Phys. Lett. **62**, 1833 (1993).

[12] J. H. Scofield, Rev. Sci. Instrum. **58**, 985 (1987); J. S. Moon, A. F. Mohamedulla, and N. O. Birge, *ibid.* **63**, 4327 (1992).

[13] Arindam Ghosh, Ph.D. thesis, Indian Institute of Science, Bangalore, India, 2000.

[14] F. N. Hoog, Physica B **83**, 14 (1976); **162**, 344 (1990).

[15] M. S. Islam, M. Cherry, and C. R. A. Catlow, J. Solid State Chem. **124**, 230 (1996), and references therein.

[16] Arindam Ghosh, A. K. Raychaudhuri, R. Sreekala, M. Rajeswari, and T. Venkatesan, Phys. Rev. B **58**, R14 665 (1998).

[17] J. Wong and C.A. Angell, *Glass Structure by Spectroscopy* (Dekker, New York, 1976).

[18] S. Hunklinger and A. K. Raychaudhuri, Prog. Low Temp. Phys. **9**, 265 (1986).

[19] T. Kyomen, M. Oguni, K. Kitayama, and M. Itoh, Phys. Rev. B **52**, 3177 (1995).

[20] M. F. Shlesinger and E. W. Montroll, Proc. Natl. Acad. Sci. U.S.A. **81**, 1280 (1984); J. Klafter and M. F. Shlesinger, *ibid.* **83**, 848 (1985).

[21] E. W. Montroll and J. T. Bendler, J. Stat. Phys. **34**, 129 (1984).